EVOLUTIONARY BIOLOGY

Convergent genomic signatures of local adaptation across a continental-scale environmental gradient

Lucas R. Moreira[1,2,3]* and Brian Tilston Smith[2]

Convergent local adaptation offers a glimpse into the role of constraint and stochasticity in adaptive evolution, in particular the extent to which similar genetic mechanisms drive adaptation to common selective forces. Here, we investigated the genomics of local adaptation in two nonsister woodpeckers that are codistributed across an entire continent and exhibit remarkably convergent patterns of geographic variation. We sequenced the genomes of 140 individuals of Downy (*Dryobates pubescens*) and Hairy (*Dryobates villosus*) woodpeckers and used a suite of genomic approaches to identify loci under selection. We showed evidence that convergent genes have been targeted by selection in response to shared environmental pressures, such as temperature and precipitation. Among candidates, we found multiple genes putatively linked to key phenotypic adaptations to climate, including differences in body size (e.g., *IGFPB*) and plumage (e.g., *MREG*). These results are consistent with genetic constraints limiting the pathways of adaptation to broad climatic gradients, even after genetic backgrounds diverge.

INTRODUCTION

Convergent local adaptation offers an opportunity to investigate the predictability of adaptive evolution to spatially heterogeneous selective pressures (*1*, *2*). When the same loci are independently used in distinct episodes of adaptation, it is likely that particular constraints exist on the number of evolutionary pathways available for adaptation (*3*). For example, some genes may contribute more often to adaptation owing to their larger phenotypic effects, lower functional redundancy, higher mutation rates, or fewer epistatic and pleiotropic interactions (*3*–*5*). Under such circumstances, closely related taxa diverging along a similar environmental gradient, such as a latitudinal cline, should exhibit some degree of genetic convergence, as natural selection will operate on a similar genomic background (*6*). On the other hand, local adaptation may evolve via different genetic mechanisms when adaptive mutations are highly redundant and genomic backgrounds differ greatly (*7*, *8*). In this case, climatic adaptation should be characterized by lineage-specific signatures of selection (*9*).

While most studies on parallel adaptation have focused on single environmental transitions [e.g., high versus low elevation; temperature gradient; marine versus freshwater environments (*10*–*12*)], little is known about the mechanisms underlying adaptation on a continental scale, encompassing multiple contrasts. Moreover, much of the knowledge of the repeatability of adaptive evolution is based on comparisons of closely related lineages, whose shared standing genetic variation leads to evolutionary nonindependence (*11*, *13*, *14*). By comparing signatures of selection across multiple environmental axes in more distantly related, nonsister species, the effects of multiple selective pressures on genomic convergence can be elucidated (*15*, *16*).

To investigate the genomic architecture of convergent local adaptation in independently evolving and widely distributed taxa, we studied the Downy Woodpecker (*Dryobates pubescens*) and Hairy Woodpecker (*Dryobates villosus*), two sympatric and ecologically similar species that co-occur across a complex environmental gradient in North America. These two species (also referred to as Downy and Hairy, for short) are year-round residents of a variety of forested habitats, including coniferous, deciduous, and mixed forests, being found from Alaska (AK) to Florida, although populations of Hairy Woodpecker are also found in Central America and The Bahamas (*17*). Over the past million years, populations of both woodpeckers have been strongly affected by the Pleistocene glaciations, experiencing repeated cycles of bottleneck and population expansion as a result of the advance and retreat of the Pleistocene glacier in North America (*18*). These changes in habitat availability during the Pleistocene led to isolation in multiple glacial refugia which, along with heterogeneous gene flow across the landscape, caused population differentiation. Despite this dynamic demographic history, Downy and Hairy Woodpeckers were able to maintain very large effective population sizes, which might have prevented erosion of adaptive variation by genetic drift and therefore facilitated the action of natural selection (*18*). Moreover, although they belong to different clades, separating more than eight million years ago (*19*, *20*), Downy and Hairy Woodpeckers resemble each other more closely than other species of their clades (*21*). This plumage convergence is hypothesized to result from interspecies social dominance mimicry, where a smaller animal mimics a larger one to scare off competitors and gain access to resources (*22*). This phenomenon is commonly seen in woodpeckers [family Picidae; (*23*–*25*)]. Both species also exhibit extensive geographic variation in plumage and body size throughout their ranges (*17*, *26*). In general, their convergent geographic variation complies with major ecogeographical rules—individuals of both species are darker in the humid west and larger in higher latitudes and elevations, a pattern often observed in North American birds (*27*, *28*). Considering that Downy and Hairy Woodpeckers have an overlapping distribution, similar ecologies, evolved in a shared landscape for a similar period of time, and exhibit convergent

[1]Department of Ecology, Evolution and Environmental Biology, Columbia University, NY, USA. [2]Department of Ornithology, American Museum of Natural History, New York City, NY, USA. [3]Program in Bioinformatics and Integrative Biology, University of Massachusetts Chan Medical School, Worcester, MA, USA.
*Corresponding author. Email: lr2767@columbia.edu

phenotypes, they provide natural evolutionary replicates to study convergent patterns of natural selection.

As Downy and Hairy Woodpeckers independently colonized previously glaciated habitats in North America, founder populations adapted to a number of environmental stressors, such as exceptionally low temperatures, seasonal food scarcity, different diets, and new pathogens and competitors. Genetic variants that allowed individuals to overcome these challenges likely increased in frequency, leaving clear signatures in the genome [i.e., selective sweeps (*29*)]. Prolonged periods of winter, in particular, present a major physiological challenge to small birds, as they must maintain high metabolic rates of energy consumption in the face of severe cold, reduced access to food, and less daylight (*30*, *31*). Traits that confer greater cold resistance (e.g., behavioral and physiological adjustments) are therefore likely to be targeted by natural selection (*32*). Downy Woodpecker basal and peak metabolic rates are significantly higher during the winter than during the summer, which indicates that individuals are capable of elevating their metabolic rates to compensate for heat loss (*31*, *33*). Body size also plays a key adaptive role—heat loss is more pronounced in smaller birds relative to larger ones due to their increased surface-to-volume ratios. Consequently, optimal body mass seems to vary according to climate (*28*). Downy and Hairy Woodpeckers fit this expectation, showing variation that follows Bergmann′s ecogeographic rule, which states that individuals in cooler climates are generally larger than conspecifics living in warmer ones (*28*, *34*, *35*).

Considering the variety of biotic and abiotic factors that impose spatially varying selective pressures on populations of the Downy and Hairy Woodpeckers, we used a suite of genomic approaches to test for signatures of local adaptation. We resequenced the whole genome of individuals of Downy and Hairy Woodpeckers to characterize the genetic basis of local adaptation and test whether the same genes/loci have been targeted by natural selection in response to a shared environment. We hypothesized that if constraints exist in the number of available pathways for adaptation, then we should observe more shared signatures of selection than expected by chance (i.e., genomic convergence). Alternatively, if multiple evolutionary solutions exist for local adaptation and outcomes of natural selection are completely contingent on past stochastic events, then we expect signatures of selection to be largely species-specific. This study explores the implications of outlier loci and genotype-environment associations (GEAs) in relation to adaptation to climate extremes, as well as variation in body size and plumage color, as these factors reflect the multidimensionality of adaptation at a continental scale. We demonstrate that genomic convergence is an important phenomenon driving adaptive evolution across broad environmental scales, and we present exciting new candidate genes putatively implicated in key phenotypic differences in local adaptation.

RESULTS AND DISCUSSION

We performed whole-genome resequencing in 140 individuals of Downy and Hairy Woodpeckers (70 samples per species) from seven geographic locations representing major bioclimatic domains in temperate North America (n = 10 individuals per population; Fig. 1 and table S1) to identify loci contributing to local adaptation. Sampled locations covered most of the climatic variation observed across the species range, characterized by multiple clines in temperature and precipitation (Fig. 1). The sequencing coverage varied from 1.4 to 12.5× (mean = 5.1×) in Downy Woodpecker and from 1.1 to 11.7× (mean = 4.5×) in Hairy Woodpecker. Our final dataset contained a total of 7,160,291 and 7,059,731 biallelic single-nucleotide polymorphisms (SNPs) in Downy and Hairy Woodpeckers, respectively.

GEA analysis uncovers shared patterns of selection in Downy and Hairy Woodpeckers

We sought to find regions of the genome that were strongly associated with environmental variables representing the complex climatic gradient of North America. To do so, we first performed a principal components analysis (PCA) on the 19 bioclimatic variables from the WorldClim database (*36*), separating variables related to temperature (BIO1 to BIO11) from the ones related to precipitation (BIO12 to BIO19). The first three principal components (PC1 to PC3) of each of these sets, explaining 94 to 98% of the total environmental variation (table S2), were retained for our GEA analysis. We then used the latent model in ANGSD-asso [association algorithm from the Analysis of Next Generation Sequencing Data software (*37*)] to test for an association between genotypes in each SNP and PC1 to PC3 of temperature and precipitation. Because the signal of selection is expected to extend to linked sites, we estimated median values of the likelihood ratio test (LRT) for windows of 50 SNPs (in increments of 10 SNPs) across the genome and applied a permutation test to find the significance threshold for each window. This conservative strategy ensured that the number of candidate loci was not inflated by linkage disequilibrium (LD), variable gene size, or spurious associations. Our results revealed multiple SNP windows correlated with environmental variables in both species (Fig. 2, figs. S1 to S4, and tables S2 and S7). In Downy and Hairy Woodpeckers, a total of 312 (0.04%) and 1924 (0.27%) SNP windows were associated with temperature variables, respectively, whereas 217 (0.03%) and 1417 (0.2%) SNP windows were correlated with precipitation variables. For temperature, most candidate SNP windows were associated with PC1 (271 in Downy), loading most heavily on cold extremes (BIO6 and BIO11), and PC2 (1445 in Hairy), loading most heavily on hot extremes (BIO5, BIO8, and BIO10). For precipitation, a large proportion of SNP windows (140 in Downy and 300 in Hairy) were associated with PC1, which loaded most strongly on annual precipitation (BIO12). In Hairy, most SNP windows (726) were correlated with PC3 of precipitation, loading most heavily on precipitation in the warmest quarter (BIO18).

We identified a total of 37 and 328 genes overlapping (or in close proximity to) candidate SNP windows for temperature in Downy and Hairy Woodpeckers, respectively. These genes represented an array of biological processes but were enriched for functions related to regulation of insulin-like growth factor (IGF) receptor signaling pathway [Gene Ontology (GO):0043567; P = 0.017 in Downy], synaptic membrane adhesion (GO:0099560; P = 0.035 in Downy), and viral entry into host cell (GO:0046718; P < 0.001 in Hairy; tables S3 and S4). Similarly, we identified a total of 24 and 270 candidate genes associated with precipitation in Downy and Hairy Woodpeckers, respectively. These genes were related to post-embryonic organ morphogenesis (GO:0048563; P = 0.047 in Downy), response to caloric restriction (GO:0061771; P = 0.047 in Downy), regulation of testosterone secretion (GO:2000843; P = 0.047 in Downy), regulation of lipid transport (GO:0032369; P =

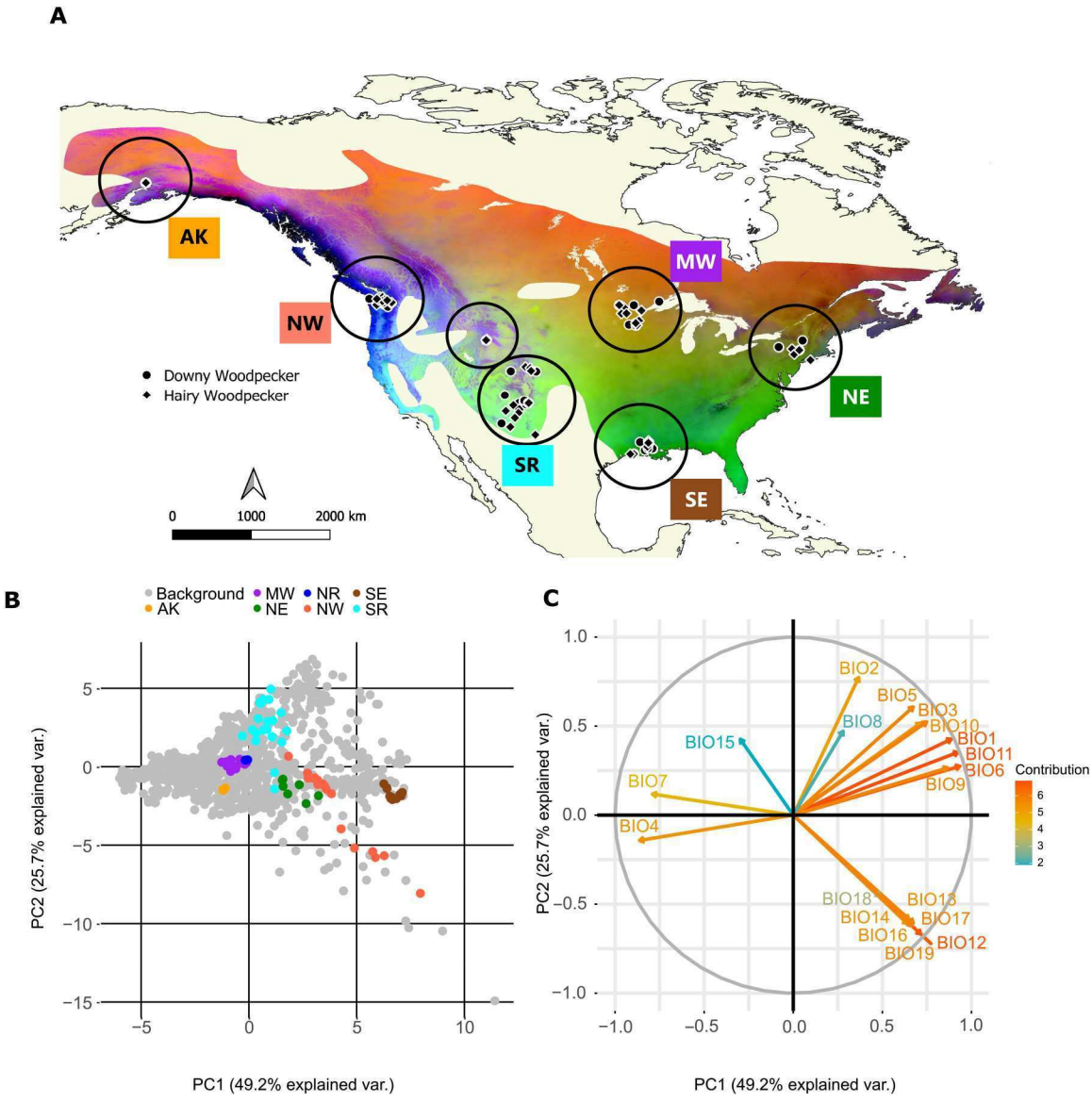

Fig. 1. Environmental variation across the ranges of Downy and Hairy Woodpeckers. (**A**) Map depicting the sympatric range of Downy and Hairy Woodpeckers, the location of the study samples (dots), and their respective populations of origin (large circles). Each population has a sample size of $n = 10$. Colors on the map are based on the principal components analysis (PCA) of the bioclimatic data shown in (B). We converted scores of the first three principal components (PCs) into values of RGB (PC1: red; PC2: green; PC3: blue) to represent variation in climate. Thus, similar colors represent similar climates. (**B**) PCA of the 19 bioclimatic variables from the WorldClim database (*36*). Background points (gray) represent 1000 randomly sampled points across the sympatric range of both focal species. Points from each population are represented by different colors. (**C**) Biplot of the PCA of bioclimatic data indicating the correlations among variables and the direction and magnitude of their contribution to the first two PCs of the PCA. AK, Alaska; MW, Midwest; NE, Northeast; NR, Northern Rockies; NW, Pacific Northwest; SE, Southeast; SR: Southern Rockies.

0.047 in Downy), polysaccharide digestion (GO:0044245; $P = 0.047$ in Downy), etc. (table S3). This diversity of gene functions suggests that, at a broad environmental scale, local adaptation involves a multitude of phenotypic, behavioral, and physiological traits, most of which have a complex genetic underpinning (*38*, *39*).

Candidate loci show signatures of selective sweep and population structure deviation

We used additional approaches to detect variants under selection to refine and validate our list of candidate loci. Because variants under selection tend to deviate from the general patterns of population structure under neutral evolution, we used the PCAdapt algorithm (*40*) to identify population structure outliers. We found 1376 outlier SNP windows in Downy and 3326 outlier SNP windows in Hairy Woodpecker deviating from the global population structure (top 1% percentile; Fig. 3, A and B). Twelve to 13% of these SNP windows overlapped with our candidate set from ANGSD-asso (Fig. 3, C and D).

Next, we searched for signatures of recent or ongoing hard sweeps using H-scan (*41*), a method that computes the average length of homozygosity tracts (H) around each SNP. For this analysis, we considered outliers, any variant window in the top 1%

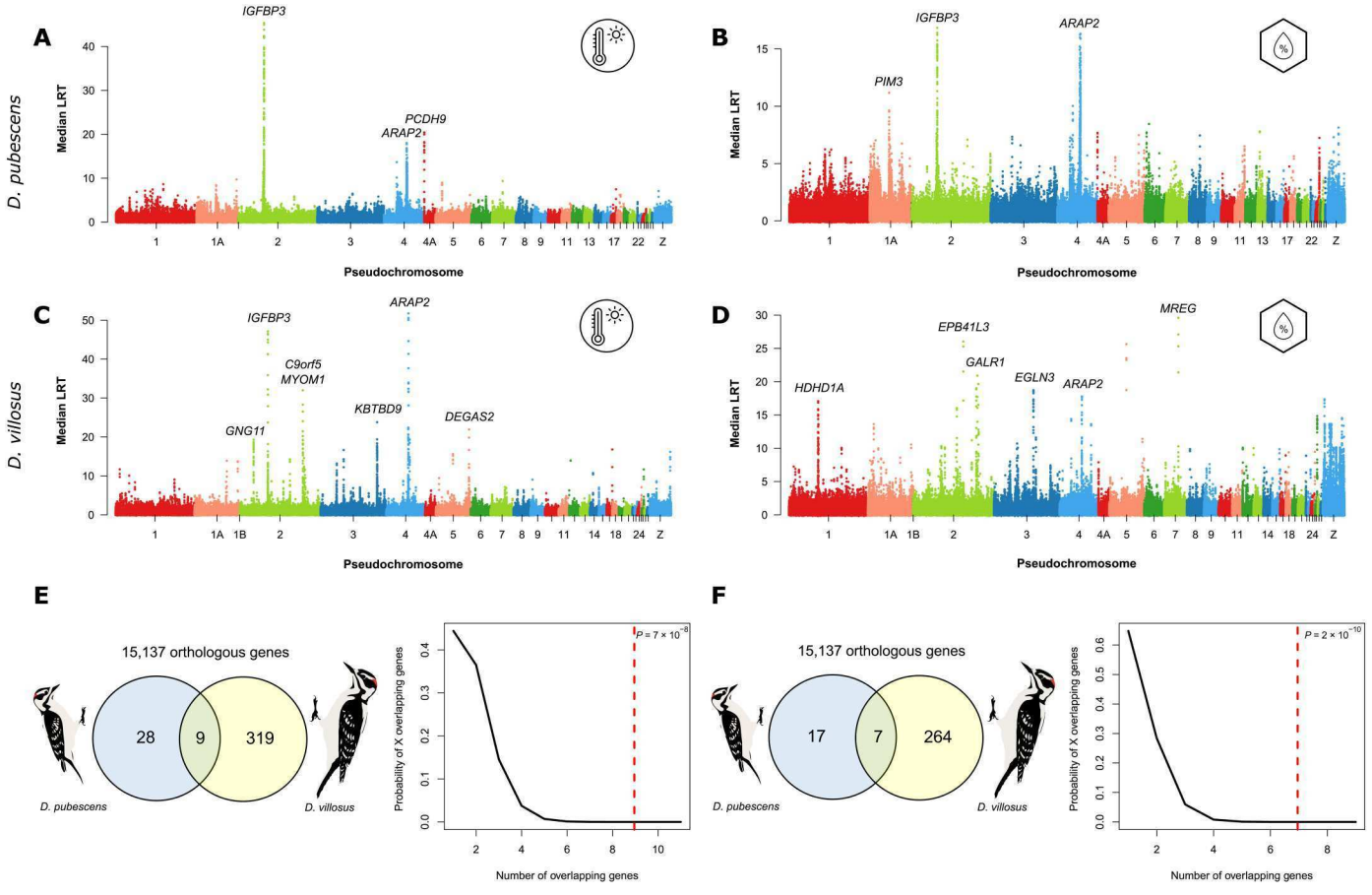

Fig. 2. GEA analysis and genomic convergence in Downy and Hairy Woodpeckers. Manhattan plots showing candidate genes associated with the first PC (PC1) of (**A**) temperature and (**B**) precipitation in Downy Woodpecker and (**C**) temperature and (**D**) precipitation in Hairy Woodpecker. Each dot represents the median LRT statistic estimated for a given 50-SNP sliding window along the genome. Colors differentiate consecutive pseudochromosomes. Venn diagram describing the total number of candidate genes from the ANGSD-asso latent model associated with (**E**) temperature and (**F**) precipitation shared by Downy (left) and Hairy (right) Woodpeckers. Density plot shows the cumulative hypergeometric distributions of the probability of observing a given number of overlapping candidate genes. The red dashed line indicates the empirical observation.

largest values of median *H*. This analysis resulted in a list of 8238 (Downy) and 10,085 (Hairy) SNP windows (figs. S5 and S6). Many of the candidate SNP windows from H-scan overlapped with candidates from ANGSD-asso (281 to 594) and PCAdapt (626 to 1648). A highly significant fraction of these SNP windows were shared between all three methods in Downy Woodpecker (188 SNP windows; $P < 0.001$; Fig. 3C) and Hairy Woodpecker (203 SNP windows; $P < 0.001$; Fig. 3D). In Downy Woodpecker, SNP windows identified by all three methods harbored genes of the IGF signaling pathway (*IGFBP3* and *IGFBP1*) and genes associated with neurodevelopment (*ADCY1*, *PCDH1*, and *PCDH9*). In Hairy Woodpecker, we identified transcription factors related to anatomical development (*BARX1*) and stress-responsive chromatin regulation (*ATF7*), as well as genes related to spermatogenesis (*CCDC65*) and melanin biosynthesis (*DCT*).

Convergent genes have been used for adaptation in Downy and Hairy Woodpeckers

We observed an overrepresentation of candidate genes under selection shared by both species. To assess the degree of genomic convergence in local adaptation to climate, we examined the overlap between candidate genes associated with climatic variables in both species. A total of nine (*GSTK1*, *TNS3*, *IGFBP1*, *IGFBP3*, *ARAP2*, *IGHV1*, *PCDH9*, and two uncharacterized) and seven (*IL17REL*, *PIM3*, *INS3*, *IGFBP3*, *ARAP2*, and two uncharacterized) shared orthologous genes were found to be associated with temperature (Fig. 2E) and precipitation (Fig. 2F), respectively. While this overlap is small, it is extremely unlikely to occur by chance, as indicated by a hypergeometric test (temperature: $P < 0.001$; precipitation: $P < 0.001$; Fig. 2, E and F, and fig. S7). These results suggest that, at the gene level, climatic adaptation was more repeatable than expected given the highly polygenic nature of adaptive phenotypes and the broad environmental scale we investigated (*16*).

Ancient introgression is unlikely to drive genetic convergence

We found limited evidence that candidate genes under selection shared by the Downy and Hairy Woodpeckers originated from adaptive introgression. While we do not have access to a more extensive taxon sampling, which would allow us to formally evaluate

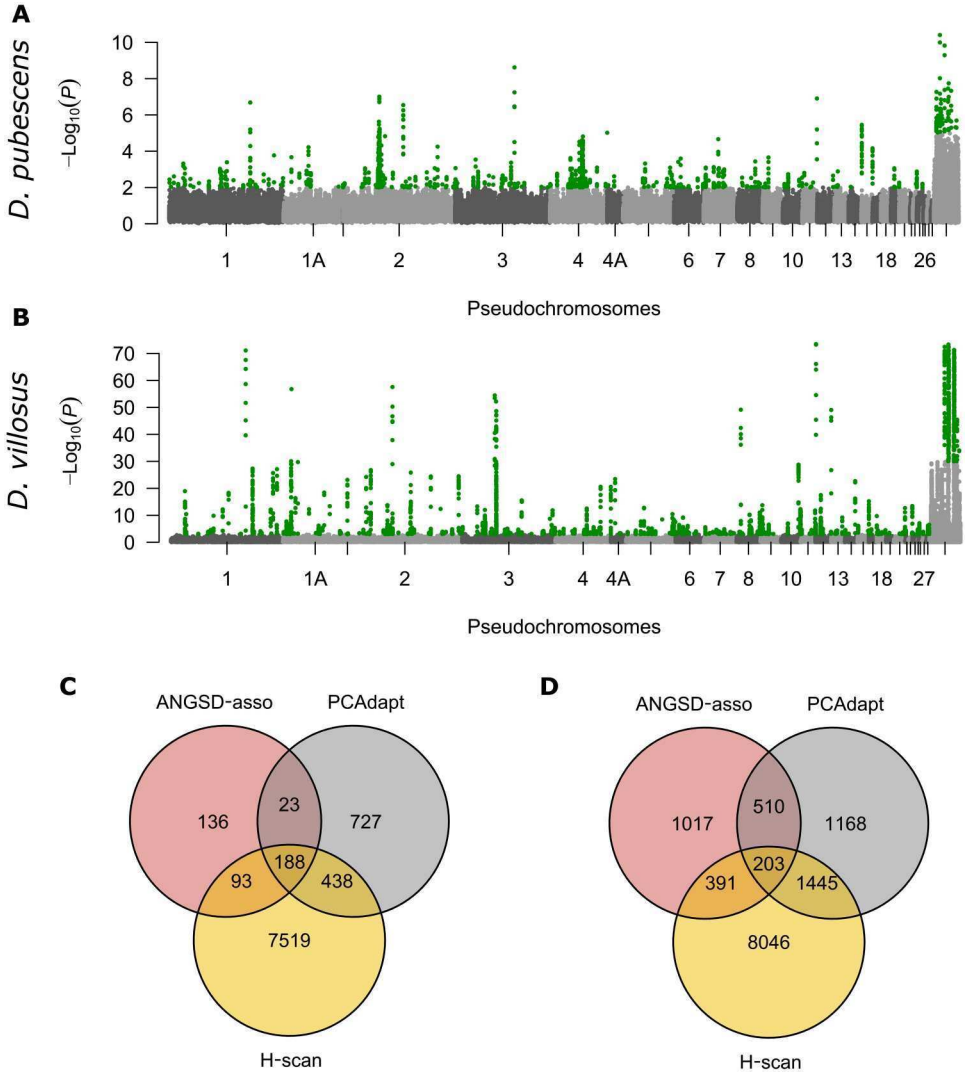

Fig. 3. Population-structure outliers and method intersection. Manhattan plots showing outliers windows of population structure according to PCAdapt in Downy (**A**) and Hairy (**B**) Woodpeckers. Each dot represents the median $-\log_{10}(P)$ estimated for a given 50-SNP sliding window along the genome. Gray colors differentiate consecutive pseudochromosomes. Green dots indicate candidate loci. Venn diagrams describing the intersection of candidate windows between ANGSD-asso, PCAdapt, and H-scan in Downy (**C**) and Hairy (**D**) Woodpeckers.

introgression, we have developed an approach to testing whether certain regions of the genome are more similar between species than within species, which could be an indication of introgression. To do so, we estimated tree topologies along the genomes of the Downy and Hairy Woodpeckers and identified genomic windows in which species monophyly was not supported (e.g., samples cluster by geography, rather than species). We identified 333 genomic windows showing nonmonophyly, which could have arisen through ancient introgression, incomplete lineage sorting, or stochasticity. However, none of these windows overlapped with candidate genes under selection in our focal species, suggesting that ancient introgression is not likely to have contributed to the observed convergence in local adaptation. Instead, our results suggest that the shared candidate genes are likely to have evolved independently in response to similar selective pressures in the two species.

Signatures of elevated genetic differentiation are associated with environmental dissimilarity

By scanning the genome of Downy and Hairy Woodpeckers, we characterized regions of elevated population differentiation (F_{ST}) when compared to the genomic background. We estimated F_{ST} across 50-kb sliding windows in 10-kb increments using the genotype likelihood approach in ANGSD (*42*). Any genomic window with an F_{ST} value 5 SDs above the genome-wide mean was considered an outlier. Given that population expansion is expected to produce exceedingly long tails in the distribution of F_{ST}, thus confounding F_{ST}-outlier analyses, we chose a conservative cutoff value, corresponding to the top 10^{-5}% of a normal distribution. Simulations have shown that this conservative cutoff performs well in other systems with nonequilibrial demographies (*12*). F_{ST}-outlier analyses across all 21 pairwise population comparisons revealed a number of outlier windows harboring candidate loci putatively under natural

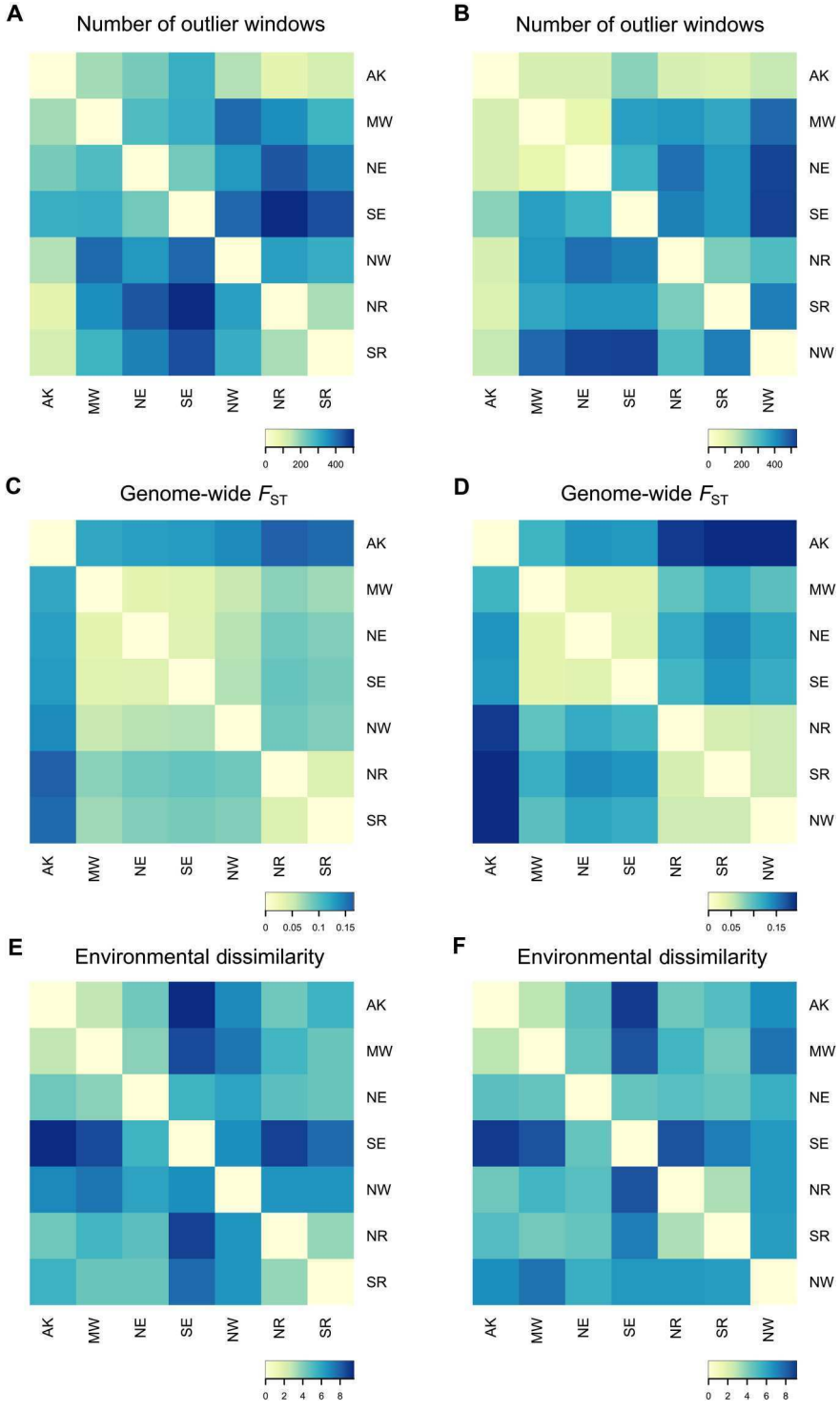

Fig. 4. Correlates of the number of F_{ST}-outlier windows in Downy and Hairy Woodpeckers. Heatmaps of F_{ST}-outlier windows and correlates across population comparisons in Downy (left) and Hairy (right) Woodpeckers. Shown are heatmaps of the number of genomic windows detected in the F_{ST}-outlier analysis for each population comparison (**A** and **B**), the genome-wide F_{ST} across all population comparisons (**C** and **D**), and the average environmental dissimilarity among populations (**E** and **F**) calculated as the Euclidean distance between PCs of the 19 bioclimatic variables from the WorldClim database (*36*). AK, Alaska; MW, Midwest; NE, Northeast; SE, Southeast; NW, Pacific Northwest; NR, Northern Rockies; SR, Southern Rockies.

selection (Fig. 4 and figs. S8 to S11). We asked whether the number of outlier windows detected in each population comparison was a function of the genome-wide F_{ST} or the average environmental dissimilarity between populations. Mantel tests revealed a correlation between the number of outlier windows and the average environmental dissimilarity (Downy: Spearman's $r = 0.5$; $P = 0.01$; Hairy: Spearman's $r = 0.42$; $P = 0.04$; Fig. 4) but not the genome-wide F_{ST} (Downy: Spearman's $r = -0.27$; $P = 0.83$; Hairy: Spearman's $r = -0.15$; $P = 0.73$; Fig. 4). The absence of a correlation between the number of outlier windows and global F_{ST} suggests that the detected candidates are likely associated with local adaptation across the broad continental-scale gradient in North America and not an artifact of higher genome-wide population differentiation.

F_{ST}-outlier analysis reveals selection on multiple genes related to the immune system and nutrition

Across all pairwise population comparisons, we found 90 to 503 (Downy Woodpecker) and 86 to 533 (Hairy Woodpecker) outlier windows showing elevated differentiation (Fig. 4, A and B). A total of 87.2 and 79% of SNP windows associated with environmental variables in Downy and Hairy, respectively, overlapped with these F_{ST}-outlier windows by at least 500 base pairs (bp). Most of these 50-kb regions harbored annotated genes—across all population comparisons, we found 572 and 610 candidate genes within regions of elevated F_{ST} in Downy and Hairy Woodpeckers, respectively. These candidate genes encompassed a broad range of molecular functions and biological processes (tables S5 and S6), including response to nutrients (e.g., *OTC*, *PHEX*, and *HMGCL*), embryonic development (e.g., *LRP6*, *ALS2*, *MEOX1*, and *OVOL2*), organism growth and maturation (e.g., *EZH2*, *IGFBP3*, and *IGFR1*), heat response (e.g., *HSP90AA1*), and melanogenesis (e.g., *RAB38*, *SHROOM2*, *ADAMTS20*, and *NF1*). These candidate genes support our findings from the GEA analysis, revealing that local adaptation is likely a complex trait that involves multiple molecular pathways.

Next, we compared candidate outlier windows in Downy and Hairy Woodpeckers and identified 217 (12.6 and 11.5%) outlier windows (with 139 annotated genes) shared between population comparisons of Downy (total unique outlier windows = 2150) and Hairy Woodpeckers (total unique outlier windows = 2355). Convergent candidate genes showed an overrepresentation of biological processes associated with immune response against pathogens (e.g., *CD36*, *TLR1B*, and *MFHAS1*; Table 1). Enriched GOs included "innate immune response in mucosa" (GO:0002227; $P < 0.001$), "antibacterial humoral response" (GO:0019731; $P = 0.019$), "defense response to Gram-positive bacterium" (GO:0050830; $P = 0.021$), "antimicrobial humoral immune response mediated by antimicrobial peptide" (GO:0061844; $P = 0.022$), and "immune system development" (GO:0002520; $P = 0.039$). Birds are thought to adjust their immune activity in response to local environment and pathogen pressure (*43*, *44*). Geographic differences in pathogen load, ecophysiology, and life history traits could explain the signatures of covergent selection for local adaptation observed in immune genes of Downy and Hairy Woodpeckers.

In addition to GO terms directly related to the immune system, we also found an overrepresentation of genes associated with nucleic acid replication, transcription, and repair in both species (Table 1). Convergent candidates were enriched for genes related to "RNA-dependent DNA biosynthetic process" (GO:0006278; $P < 0.001$), "DNA-templated transcription" (GO:0006352; $P < 0.001$), "nucleosome assembly" (GO:0006334, $P < 0.001$), "DNA integration" (GO:0015074, $P = 0.006$), and "RNA phosphodiester bond hydrolysis, endonucleolytic" (GO:0090502, $P = 0.03$). Pathways related to DNA replication and repair are significantly enriched for positively selected genes in birds (*45*) and might be indirectly related to immune response against viruses, which are known to subvert the DNA/RNA replication and repair machinery to promote their own replication (*45*). These genetic mechanisms could also have evolved in response to transposable elements (TEs), repetitive DNA sequences that have the ability to move across the genome (*46*). Woodpeckers, in particular, show a large expansion in the number of TEs, especially chicken repeat 1 retrotransposon (CR1), compared to other bird lineages, which are known for the paucity of TEs (*47*). TEs can cause deleterious effects on their "hosts" due to the disruption of gene expression by random insertions, synthesis of deleterious RNAs or proteins, or chromosomal rearrangements caused by ectopic recombination between nonallelic copies (*46*). Thus, selection is expected to operate by removing TEs from the genome, leading to a host-parasite evolutionary arms race. Consistent with this hypothesis, a study found evidence of purifying selection against polymorphic TEs in Downy Woodpecker and two other closely related species (*47*). However, TEs can also be co-opted for adaptive purposes, such as supplying regulatory elements (e.g., promoter and cis-regulatory elements) and modulating gene expression, a process known as "TE gene domestication" (*46*). In *Drosophila*, for example, TEs play a key role in adaptation to temperate climates (*48*). Candidate genes involved in retrotranscription and DNA integration suggest that TEs could have an adaptive value in Downy and Hairy Woodpeckers and might be under disruptive selection across their broad environmental distribution.

An array of processes underlie adaptation at the range peripheries

To more narrowly explore the genomic architecture of local adaptation, we focused on a key population comparison that provided an opportunity to understand adaptation at the range peripheries. We investigated signatures of selection in the comparison between AK and the Southeast (SE), the two latitudinal extremes of the sympatric distribution of the focal species, occupying opposite ends of the environmental space (Fig. 1B). This comparison revealed many candidate genes with elevated genetic differentiation compared to the genomic background (Fig. 5 and Table 2). Candidates included several genes related to immune response, such as G-protein coupled receptor 1 (*GPR1*) and C-C motif chemokine 20 (*CCL20*), both involved in the inflammation-associated chemotaxis response of several immune cells (*49*, *50*). The analysis also identified genes related to amino acid and lipid metabolism (e.g., *GADL1* and *DEGS2*), and both the pancreatic and hepatic α-amylase genes (*AMY*), enzymes that play a key role breaking down long-chain polysaccharides. Studies show that passerine birds fed with a starch-rich diet exhibit higher pancreatic amylase activities (*51*), and birds with a diet richer in seeds show higher values of dN/dS (ω) in amylase genes, suggesting positive selection for enzymatic efficiency (*52*). Populations of the House Sparrow (*Passer domesticus*) adapted to the urban environment also exhibit signatures of selection in the amylase alpha 2 [*AMY2A*; (*53*)]. Thus, differences in consumption of polysaccharides between populations of Downy

Table 1. Enriched GOs for convergent F_{ST}-outlier genes across all pairwise population comparisons. Significance was determined through a Fisher's exact test and false discovery rate correction. MAPK, mitogen-activated protein kinase; NADPH, reduced form of nicotinamide adenine dinucleotide phosphate.

GO ID	GO description	Candidate count	Genome count	Odds ratio	Corrected *P* value
GO:0002227	Innate immune response in mucosa	45	800	8.14	1.82×10^{-19}
GO:0006082	Organic acid metabolic process	8	18	82.72	9.96×10^{-10}
GO:0006278	RNA-dependent DNA biosynthetic process	10	42	32.81	1.67×10^{-09}
GO:0006334	Nucleosome assembly	9	42	28.40	3.98×10^{-08}
GO:0006342	Chromatin silencing	7	23	44.91	2.21×10^{-07}
GO:0006352	DNA-templated transcription	8	84	10.85	0.0001
GO:0006508	Proteolysis	4	13	44.63	0.0004
GO:0006805	Xenobiotic metabolic process	4	13	44.63	0.0004
GO:0006970	Response to osmotic stress	3	8	59.77	0.0030
GO:0007190	Activation of adenylate cyclase activity	3	8	59.77	0.0030
GO:0008210	Estrogen metabolic process	4	24	20.09	0.0045
GO:0009404	Toxin metabolic process	3	11	37.40	0.0067
GO:0015074	DNA integration	3	11	37.40	0.0067
GO:0015671	Oxygen transport	3	12	33.25	0.0076
GO:0017144	Drug metabolic process	3	12	33.25	0.0076
GO:0019731	Antibacterial humoral response	3	17	21.36	0.0190
GO:0032496	Response to lipopolysaccharide	3	17	21.36	0.0190
GO:0035093	Spermatogenesis, exchange of chromosomal proteins	2	4	98.89	0.0190
GO:0042744	Hydrogen peroxide catabolic process	6	106	6.08	0.0208
GO:0043086	Negative regulation of catalytic activity	10	303	3.51	0.0217
GO:0043408	Regulation of MAPK cascade	4	43	10.29	0.0217
GO:0043567	Regulation of IGF receptor signaling pathway	8	194	4.40	0.0217
GO:0050830	Defense response to Gram-positive bacterium	3	19	18.70	0.0217
GO:0051552	Flavone metabolic process	3	20	17.60	0.0217
GO:0052696	Flavonoid glucuronidation	2	5	65.86	0.0217
GO:0052697	Xenobiotic glucuronidation	2	5	65.86	0.0217
GO:0061844	Antimicrobial humoral immune response mediated by antimicrobial peptide	4	45	9.79	0.0222
GO:0070980	Biphenyl catabolic process	3	21	16.62	0.0232
GO:0070995	NADPH oxidation	2	6	49.47	0.0283
GO:0072592	Oxygen metabolic process	4	50	8.72	0.0297
GO:0090502	RNA phosphodiester bond hydrolysis, endonucleolytic	8	218	3.89	0.0300
GO:0098869	Cellular oxidant detoxification	3	24	14.25	0.0303
GO:1990418	Response to IGF stimulus	2	7	39.61	0.0345

Woodpecker in AK and the SE might impose substantial selective pressures on enzymatic genes. In addition, several candidate genes were associated with embryonic development, such as vitellogenin 3 (*VTG3*), a gene that expresses the precursor of the egg-yolk proteins, an essential source of nutrients in the early stages of bird development (*54*). Other genes were related to mitochondrial maintenance and respiration (e.g., *NDFS1*, *FASTKD5*, and *MRPL44*). Downy Woodpecker's ability to elevate its metabolic rate to compensate for heat loss is expected to be accompanied by an elevated mitochondrial activity and could lead to different selective pressures on mitochondrial efficiency (*31*, *33*).

Convergent selection on the IGF signaling pathway is putatively associated with body size

We found convergent signatures of selection at genes of the IGF signaling pathway in comparisons involving small- versus large-bodied populations of Downy and Hairy Woodpeckers. The largest F_{ST} peak in the comparison between AK and the SE was located in the pseudochromosome 2 between 50 and 55 Mb (Fig. 5C). This peak contained several genes (some of which have been discussed in the previous paragraphs), but the largest values of F_{ST} were found in proximity to two IGF-binding proteins (IGFBPs)—*IGFBP1* and *IGFBP3* (Fig. 5C). IGFBPs are a highly

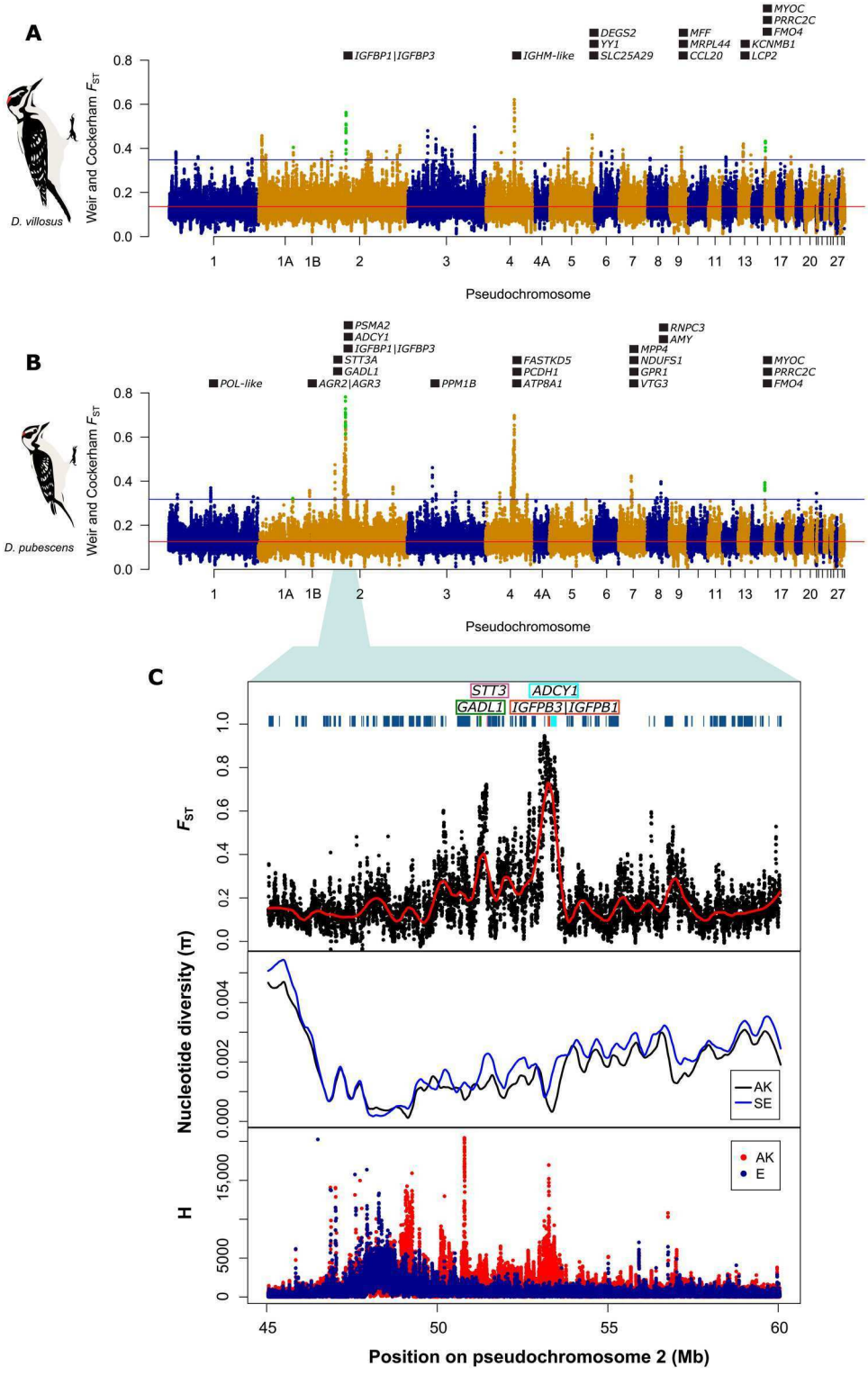

Fig. 5. IGFBP genes show convergent signatures of selection in Downy and Hairy Woodpeckers. Manhattan plot comparing Alaska (AK) and the Southeast (SE) population in (**A**) Downy and (**B**) Hairy Woodpeckers. Each dot represents the F_{ST} value estimated for a given 50-kb sliding window along the genome. Colors differentiate consecutive pseudochromosomes. The red line indicates the genome-wide mean F_{ST} (Downy F_{ST} = 0.12; Hairy F_{ST} = 0.13), and the blue line indicates the cutoff value of 5 SDs above the mean for a window to be considered an outlier (Downy F_{ST} = 0.32; Hairy F_{ST} = 0.34). Squares indicate the location of key annotated genes found within outlier windows. (**C**) Genomic signatures of selective sweep in the comparison between AK and the SE in a segment of pseudochromosome 2 of Downy Woodpecker. Top: F_{ST} between AK and the SE across 10-kb windows in 2-kb increments. The red line represents the local polynomial regression fit, and the blue rectangles indicate the location of genes. Five key genes with elevated F_{ST} are indicated by different colors. Middle: Nucleotide diversity in AK (black line) and the SE (blue line). Bottom: Average length of pairwise homozygosity tracts for each SNP (H) along this segment of pseudochromosome 2 in the AK (red) and Eastern (blue) population. E, East (NE + SE + MW).

Table 2. Candidate genes within windows of elevated F_{ST} in the comparison between AK and the SE. D, Downy Woodpecker; H, Hairy Woodpecker; B, both.

Pseudochromosome	Gene	Protein	General function	Spp.*
2	*AGR2/ AGR3*	Anterior gradient protein homologs 2 and 3	Production of mucus and regulation of intracellular calcium in tracheal epithelial cells	D
2	*GADL1*	Acidic amino acid decarboxylase	Decarboxylation of amino acids	D
2	*STT3A*	Dolichyl-diphosphooligosaccharide-protein glycosyltransferase	Protein glycosylation	D
2	*IGFBP1/ IGFBP3*	Insulin-like growth factor binding proteins 1 and 3	Regulation of growth, cell proliferation, muscular development, response to stress, and body size	B
2	*RSPO2*	R-spondin 2	Limb specification during embryonic development	H
2	*PSMA2*	Proteasome subunit alpha type 2	Maintenance of protein homeostasis; immune system	D
3	*PPM1B*	Protein phosphatase 1B	Regulation of immune response to infection and stress	D
4	*ATP8A1*	Phospholipid-transporting ATPase IA	Aminophospholipid translocase at the plasma membrane; involved in brain connectivity	D
4	*RELL1*	RELT-like protein 1	Activation of the MAPK14/p38 cascade; response to stress	D
4	*PCDH1*	Protocadherin 1	Cell-cell interactions and cell adhesion	D
4	*FASTKD*	FAST kinase domain-containing protein 2	Processing of non-canonical mitochondrial mRNA precursors	D
5	*DEGS2*	Sphingolipid delta(4)-desaturase/C4-monooxygenase	Sphingolipid biosynthesis	H
5	*YY1*	Transcriptional repressor protein YY1	Development and differentiation	H
5	*SLC25A29*	Mitochondrial basic amino acids transporter	Mitochondrial basic amino acids transporter	H
7	*NDUFS1*	NADH-ubiquinone oxidoreductase 75-kDa subunit	Core subunit of the mitochondrial membrane respiratory chain NADH dehydrogenase	D
7	*GPR1*	G protein–coupled receptor GPR1	Receptor for the inflammation-associated leukocyte chemoattractant; regulation of inflammation; detection of glucose	D
7	*EEF1B2*	Elongation factor 1-beta	Translation elongation	D
7	*VTG3*	Vitellogenin 3	Precursor of the egg-yolk proteins	D
7	*MPP4*	MAGUK p55 subfamily member 4	Retinal photoreceptors development	D
7	*ALS2CR4*	Transmembrane protein 237	Ciliogenesis	D
8	*AMY1/ AMY2*	Alpha amylase	Polysaccharide endohydrolysis (digestive enzyme)	D
9	*MFF*	Mitochondrial fission factor	Mitochondrial and peroxisomal fission	H
9	*MRPL44*	39*S* ribosomal protein L44	Component of the 39*S* subunit of mitochondrial ribosome	H
9	*SLC19A3*	Thiamine transporter 2	Thiamine transporter	H
9	*CCL20*	C-C motif chemokine 20	Chemotaxis of immune cells at skin and mucosal surfaces	H
13	*KCNMB1*	Calcium-activated potassium channel subunit beta-1	Regulatory subunit of the calcium activated potassium KCNMA1 (maxiK) channel	H
13	*LCP2*	Lymphocyte cytosolic protein 2	T cell antigen receptor mediated signaling	H
15	*MYOC*	Myocilin	Regulation of cell adhesion, cell-matrix adhesion, cytoskeleton organization and cell migration; bone formation; muscle hypertrophy; neurite outgrowth	B
15	*PRRC2C*	BAT2 domain-containing protein 1	Formation of stress granules	B
15	*FMO4*	Dimethylaniline monooxygenase	Metabolism of xenobiotics	B

*Species in which the candidate gene was detected.

conserved family of proteins that bind to IGFs, especially IGF-1, to assist their transport around the body and prolong their half-lives (*55*). It is well known that IGF-1 plays a crucial role stimulating growth, differentiation, and proliferation of cells, thereby mediating the overall postnatal growth rate and body size of various vertebrates (*56*, *57*). IGF-1 has been linked to several metabolic and developmental pathways, including muscle mass growth, remodeling of skeletal tissue, neurogenesis of the nervous system, and nutrient metabolism (*58*–*60*). In the chicken, higher expression and plasma levels of IGF-1 were correlated with larger body weight (*56*), and in ovo injections of IGF-1 resulted in increased body sizes (*61*). Other studies found a positive association between IGF-1 levels and body size both across and within passerine species (*62*, *63*) and revealed that levels of IGF-1 are associated with life-history strategies (*64*) and expression of plumage traits (*65*).

We found that across 12 population comparisons in Downy Woodpecker and 11 in Hairy Woodpecker, the genomic region harboring the *IGFBP1* and *IGFBP3* genes shows exceedingly large genetic differentiation when compared to the genomic background (figs. S8 to S11). In both species, an F_{ST} peak was evident across all comparisons between the SE and any other population. This genomic region was also an outlier in the comparisons between the Northeast (NE) and other western populations [e.g., Northern Rockies (NR), Pacific Northwest (NW), and AK], and in Hairy Woodpecker, in the comparisons between the Midwest (MW) and other western populations. The region of pseudochromosome 2 containing *IGFBP1* and *IGFBP3* was also characterized by low nucleotide diversity and extended homozygosity, genomic signatures of a selective sweep (Fig. 5C). In addition, these genes show a strong association with climatic variables, especially temperature (Fig. 2). Body sizes in both species are known to change clinally with latitude—birds in higher latitudes and elevations (e.g., AK and NR) are larger than their southern counterparts [e.g., SE; (*17*)]. This pattern conforms to the Bergmann's rule, where individuals in cooler climates tend to be larger than conspecifics in warmer areas (*66*), and might indicate that Downy and Hairy Woodpeckers have evolved larger bodies to conserve heat in areas where temperatures are lower (*67*, *68*). Our results show that an elevated F_{ST} in the genomic region harboring *IGFBP1* and *IGFBP3* was observed in all comparisons between populations of small versus large birds. We hypothesize that these candidate genes contribute to differences in body size across populations and have been under convergent natural selection in both species.

Hemoglobin genes show signatures of convergent selection in high-elevation populations

High-elevation populations of Downy and Hairy Woodpeckers show convergent signatures of selection in hemoglobin genes. Across our set of candidate genes for convergent local adaptation, we also found that genes associated with "oxygen transport" (GO:0015671, $P < 0.001$) and "gas transport" (GO:0015669, $P < 0.001$) were overrepresented. Population comparisons between highland [NR and Southern Rockies (SR)] and lowland (e.g., SE and NW) show outlier values of F_{ST} in a region of pseudochromosome 1 between 20.75 and 20.80 Mb and a region of pseudochromosome 14 between 5.80 and 5.82 Mb (figs. S8 to S11). Both regions harbor a cluster of genes that encode for the β- and α-type subunits of hemoglobin, the protein responsible for carrying oxygen through the bloodstream of most vertebrates (*69*). In woodpeckers, the β-globin cluster in pseudochromosome 1 contains three genes arranged in tandem—*Hbb*-ρ, *Hbb*-β^A, and *Hbb*-ε, and two pseudogenes—*pseudo-Hbb*-β^H and an unactivated version of *Hbb*-ε (*70*). Although an adaptive increase in oxygen affinity in high-altitude birds is often associated with (sometimes predictable) amino acid changes in these hemoglobin proteins (*71*, *72*), we did not find nonsynonymous mutations that could be linked to differences in allele frequencies in high-elevation in these woodpeckers, as most candidate SNPs were located in pseudogenes. However, we cannot discard the possibility that selection on regulatory and/or structural variants could underlie differences between lowland and highland populations.

Melanoregulin is a candidate for plumage variation in Hairy Woodpecker

Another component of convergent adaptation in Downy and Hairy Woodpeckers is their covariance in plumage color. In both species, western birds tend to be darker than their eastern counterparts (*17*). We found a very conspicuous F_{ST} peak in pseudochromosome 7 (between 20.2 and 20.5 Mb) in all comparisons between the Pacific NW and any other population of the Hairy Woodpecker (Fig. 6). This genomic region includes the gene melanoregulin (*MREG*), a gene implicated in hair and skin pigmentation in mammals (*73*, *74*). In mice, melanoregulin mediates the transfer of melanin from melanocytes (the cells that synthesize melanin) to keratocytes (the main cells of skin and hair). Our results indicate that *MREG*, a gene poorly explored in the avian literature, might be a potential candidate for plumage color. In birds, the particular location and timing of this transfer during feather development are thought to produce unique pigmentation patterns (*75*). Individuals of both Downy and Hairy Woodpeckers in the NW population are much darker than individuals from other populations sampled in this study. Our results revealed exceedingly large F_{ST} values near the *MREG* gene and evidence of a selective sweep in this population, characterized by exceedingly long tracts of homozygosity and several fixed variants (Fig. 6, B and C) in the NW population of Hairy Woodpecker. In addition, we found a strong association between the *MREG* gene and precipitation (Fig. 2D). This candidate region was absent in Downy Woodpecker (figs. S8 to S11), suggesting that, although convergent, plumage variation in Downy and Hairy might have different genetic origins. If plumage color is an adaptive trait, then the finding of different genetic underpinnings despite the overarching genetic convergence in local adaptation indicates that phenotypic convergence can still be achieved through species-specific molecular mechanisms.

In conclusion, convergent local adaptation provides a unique opportunity to understand how natural selection operates in independent evolutionary lineages. In particular, genomic data allow for the exploration of whether selective constraints limit the total number of genetic avenues available for adaptation, leading to genomic repeatability. We investigated convergent local adaptation in Downy and Hairy Woodpeckers, two species codistributed across a highly heterogeneous environmental gradient in North America. Our results revealed that despite the large evolutionary distance between the two species, natural selection targeted convergent genetic mechanisms for local adaptation. Our genotype-environment analysis identified SNP windows exhibiting a strong association with temperature and precipitation. This correlation suggests

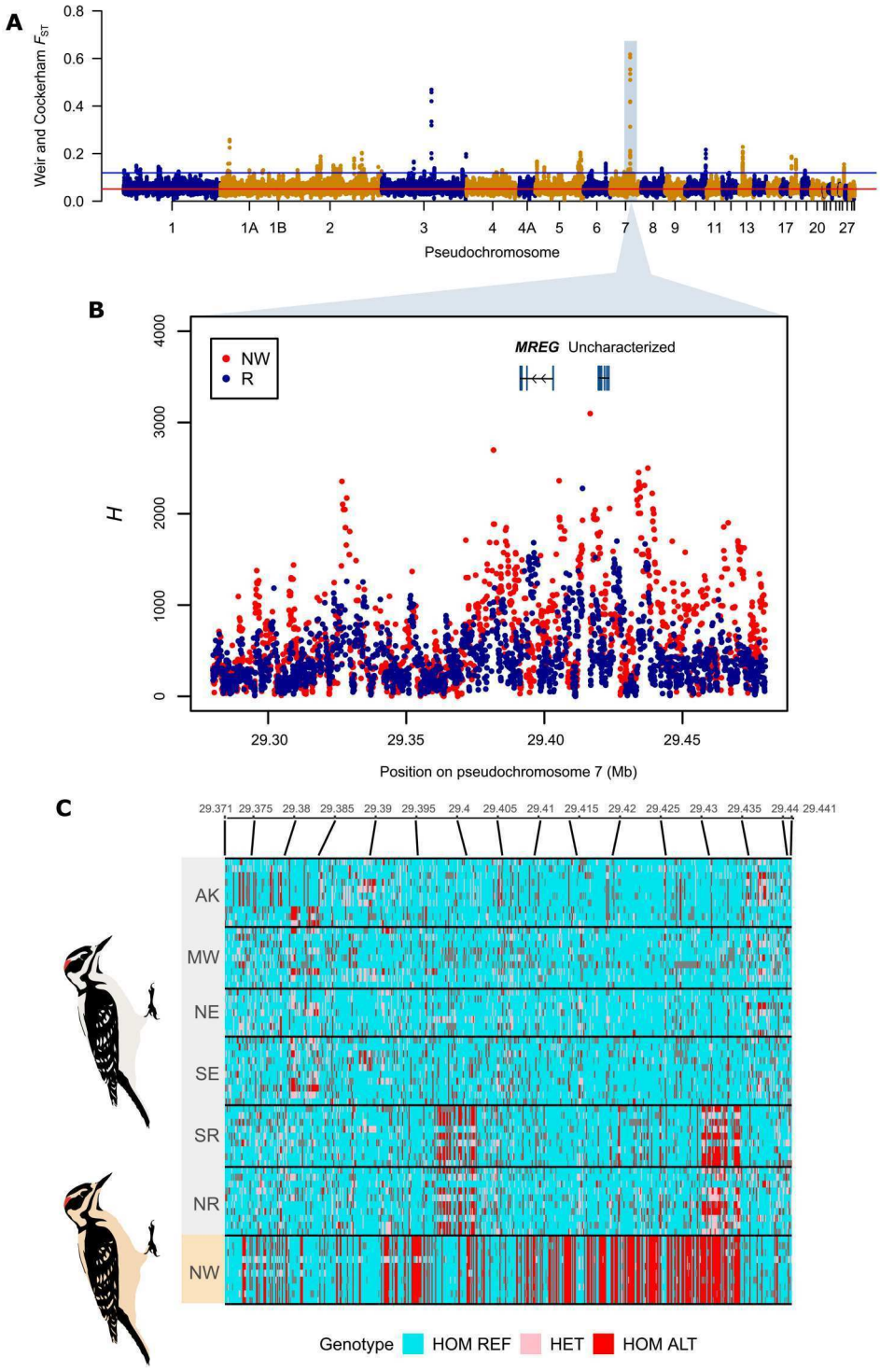

Fig. 6. A candidate gene for plumage variation in Hairy Woodpecker. (**A**) Manhattan plot showing F_{ST} values between Pacific Northwest (NW) and NR estimated for 50-kb sliding windows along the genome with 10-kb increments. Colors differentiate consecutive pseudochromosomes. The red line indicates the genome-wide mean F_{ST} (F_{ST} = 0.05), and the blue line indicates the cutoff value of 5 SDs above the mean for a window to be considered outlier (F_{ST} = 0.11). (**B**) Average length of pairwise homozygosity tracts for each SNP (*H*) for the NW (dark individuals) and NR (white individuals) population in a segment of pseudochromosome 7 containing the gene melanoregulin (*MREG*). (**C**) Genotypes for each SNP located in the segment containing the *MREG* gene separated by population. Blue, homozygous for the reference allele; pink, heterozygous; red, homozygous for the alternative allele; brown, missing genotype. AK, Alaska; MW, Midwest; NE, Northeast; SE, Southeast; SR, Southern Rockies; NR, Northern Rockies; NW, Northwest.

that climatic variables impose strong selective pressures (either directly or indirectly) across both species' ranges. We detected several candidate genes exhibiting signatures of natural selection (e.g., elevated population differentiation and extended homozygosity) in Downy and Hairy Woodpeckers. These candidate genes were involved in a broad array of biological processes, including embryonic development, nutritional metabolism, mitochondrial respiration, and oxygen transportation. Among the shared candidates, we found an overrepresentation of genes related to DNA replication and immune response, both of which are linked to defense mechanisms against region-specific pathogens. Our genomic scan for selection also identified potential candidates associated with key phenotypic traits in both focal taxa. For example, signatures of selective sweep around the melanoregulin gene (*MREG*) in a darker-plumage population of Hairy Woodpecker suggest its role in plumage variation. In addition, convergent signatures of selection in genes belonging to the IGF signaling pathway were consistent with differences in body size among population comparisons. Together, these results provide compelling evidence that, across multiple axes of environmental variation, adaptation tends to be reached through common genetic pathways more often than different ones, even when species diverge for over eight million years.

MATERIALS AND METHODS

Sample acquisition and whole genome sequencing

Seventy samples of Downy (*D. pubescens*) and Hairy Woodpeckers (*D. villosus*) each were collected in seven geographic locations (referred to as populations) consisting of major bioclimatic domains of temperate North America (n = 10 per population; Fig. 1): New York (NE), Louisiana (SE), Minnesota (MW), New Mexico and Colorado (SR), Wyoming (NR), Washington (NW), and AK. Tissue samples from museum-vouchered specimens were acquired by targeted field expeditions conducted in Wyoming, Louisiana, and AK and supplemented by loans from natural history museums (table S1). All required U.S. Federal and State permits to collect specimens specifically used in this study were obtained from the appropriate agencies. Genomic DNA was extracted from tissue samples using the MagAttract High Molecular Weight DNA Kit from Qiagen following the manufacturer's instructions (Qiagen, CA, USA). Extracted DNA was submitted for whole-genome resequencing on a paired-end Illumina HiSeq X Ten machine by RAPiD Genomics (Gainesville, FL, USA).

Read alignment, variant calling, and filtering

We removed adapters, trimmed low-quality ends, and filtered raw reads using Trimmomatic v0.36 (*76*), resulting in an average of 35,689,979 paired reads per sample. Read quality was verified using FastQC v0.11.4. (*77*). Processed reads were then mapped against the pseudochromosome reference genome of Downy Woodpecker using the Burrows-Wheeler Aligner (BWA) v0.7.15 mem algorithm (*78*) following the procedures described in detail in (*18*). We converted the resulting sequence alignment/map (SAM) files to their binary format (BAM), added sequence group information, sorted, marked for duplicates, and indexed using Picard (http://broadinstitute.github.io/picard/). We then used IndelRealigner, part of the Genome Analysis Toolkit [GATK v3.6 (*79*)], to correct read alignment errors near insertion and deletion (indels). The quality of mapping was assessed using QualiMap v.2.2.1 (*80*).

We used ANGSD v0.917 (*42*) to detect polymorphic sites and infer genotype likelihoods while integrating over the uncertainty associated with low-depth sequencing data. We estimated genotype likelihoods from aligned BAM files using the GATK model [-GL 2; (*81*)], estimating allele frequencies directly from genotype likelihoods assuming known major and minor alleles (*-doMajorMinor 1 -doMaf 1*). We retained only sites with <30% missing data (*-minInd 50*), a minimum frequency of the minor allele of 5% (*-minMaf 0.05*), a minimum mapping quality of 30 (-minMapQ 30), a minimum quality score of 20 (-minQ 20), and a P value threshold for the allele-frequency LRT statistic of 1×10^{-6} (-SNP_pval $1e^{-6}$). This resulted in a final dataset of 7,160,291 and 7,059,731 SNPs in Downy and Hairy Woodpeckers, respectively. Last, we used snpeff v4.1 (*82*) to annotate the functional impact of each SNP, according to the gene annotation of Downy Woodpecker [National Center for Biotechnology Information (NCBI) RefSeq GCF_000699005.1].

GEA analysis

We performed a GEA analysis to search for SNPs whose genotypes showed a direct association with the bioclimatic variables extracted from the Worldclim database (*36*). To reduce the collinearity among the 19 environmental variables, we performed a PCA using the R function *prcomp* separating two sets of variables—one set representing temperature (BIO1 to BIO11) and another set representing precipitation (BIO12 to BIO19). All variables were centered and scaled before the PCA. We retained the first three PCs (PC1 to PC3; temperature = 95% variance explained; precipitation = 98% variance explained) to summarize the variation in these two sets of variables. We then used the latent model in ANGSD-asso to test for an association between genotypes in each site and PC1 to PC3 of temperature and precipitation (*37*). This method accounts for the genotype uncertainty by modeling the unobserved genotype as a latent variable in a generalized linear model framework. Before running the GEA analysis, we performed an imputation of missing data using genotype likelihoods from ANGSD in Beagle v3 (*83*). Next, we ran GEA using the latent genotype model (EM algorithm; *-doAsso 4*) with the genome-wide PC1 to PC3 scores from PCAngsd (*84*) as covariates to control for population structure (*-cov*).

In GEA studies with dense SNP datasets that are not pruned for LD, individual SNPs may produce noisy estimates of association, potentially resulting in a large number of false positives (*85*). However, SNPs in close proximity often exhibit correlated patterns of association due to their nonindependent inheritance (genetic linkage). To leverage this linkage information, recent approaches have aggregated data across multiple adjacent sites through the use of window-based analyses (*85*, *86*). These approaches have the advantage of increasing statistical power and improving the signal-to-noise ratio (*29*). Thus, we obtained median LRT statistics (following a χ^2 distribution with one degree of freedom) for sliding windows of 50 SNPs, with a step size of 10 SNPs, using the R package WindowScanR (*87*). To determine a threshold of significance, we first produced a null distribution of LRT for each individual SNP by repeating the GEA analysis 200 times while randomly permutating the environmental data in each run. We considered a sliding SNP window significant when the median LRT-statistic value was above the 99.99th percentile of the null distribution.

To test for convergence in a set of genes, we calculated the probability of observing a given number of overlapping candidates under a hypergeometric distribution, if genes were randomly drawn from a total pool. Following (*6*), we used the *phyper* and *dhyper* functions in R to calculate significance and plot the cumulative distributions, respectively.

Signatures of selective sweep

We investigated signatures of selective sweep by calculating, for each SNP in each genetic cluster (AK, East, Rocky Mountains, and Pacific NW), the *H* statistic implemented in H-scan (*41*). This metric measures the average length of pairwise homozygosity tracts around a given focal SNP and, in contrast to other methods that search for genomic signatures of selective sweeps, it does not require phased haplotypes. Recent or ongoing selective sweeps are expected to show elevated LD around the target of selection, producing exceedingly long tracts of homozygosity. If genes showing atypically high F_{ST} or a strong association with environmental variables have undergone a hard sweep, linked SNPs are expected to exhibit large values of the *H* within specific populations. We ran H-scan using genotype calls from GATK v3.8.0 (*79*). We first used the HaplotypeCaller algorithm separately for each sample using the following options: *--emitRefConfidence GVCF -minPruning 1 -minDanglingBranchLength 1*. We then jointly called genotypes across all genomic variant call format (gVCF) files using GenotypeGVCFs with default settings. We followed the hard filtering recommendations from the Broad Institute′s Best Practices (https://gatk.broadinstitute.org/) to remove SNPs with annotations values above or below the following thresholds: QualByDepth (QD) < 2.0, ReadPosRankSum < −80, FisherStrand (FS) > 60.0, StrandOddsRatio (SOR) > 3.0, RMSMappingQuality (MQ) < 40.0, and MQRankSumTest < −12.5. Last, we used VCFtools v0.1.17 (*88*) to retain only biallelic SNPs meeting the following criteria: (i) missing data < 25% across all samples, (ii) read depth between 2× and 50×, and (iii) minor allele frequency (maf) > 0.05. We considered candidates of selective sweeps, all 50-SNP sliding windows (with a window step of 10 SNPs) in the top 1% quantile of *H* values.

Population structure outliers

To scan the genome for loci deviating from the neutral population structure, we used the PCAdapt algorithm implemented in ANGSD (*40*). PCAdapt computes Mahalanobis distances to measure the extent to which every SNP in the dataset is related to the first K PCs of the genetic variation. SNPs under selection are expected to show strong deviation (i.e., large Mahalanobis distances) from the general population structure. We considered outliers any sliding window of 50 SNPs (with a window step of 10 SNPs) with exceptionally high Mahalanobis D^2 distances from the vector of *z*-scores, as represented by the bottom 1% percentile of *P* values (estimated separately for autosomal and sex chromosomes). Statistical significance was obtained from a χ^2 distribution with degrees of freedom equal to the number of PCs. We lastly identified overlapping SNP windows across methods and evaluated their statistical significance using a simulation approach. Specifically, we generated a null distribution of the expected number of overlaps by randomly selecting candidate windows from the genomic pool equal in number to the empirical results of each method and repeating this process 1000 times.

F_{ST}-outlier analysis

To detect signatures of selection associated with differences in allele frequencies between populations, we estimated F_{ST} across 50-kb sliding windows with a window step of 10 kb using ANGSD v0.917 (*42*). ANGSD estimates F_{ST} using genotype likelihoods instead of relying on genotype calls. For this analysis, we first estimated allele frequencies directly from genotype likelihoods assuming known major and minor alleles [*-doSaf* 1 *-doMajorMinor* 1 *-doMaf* 1; (*89*)] and using only variants meeting the following quality filter criteria: -minMapQ 30, -minQ 20, -minMaf 0.05, and -SNP_pval 0.01. A detailed explanation of these filters can be found in (*18*). The resulting site-allele-frequency likelihood files were then used to generate a folded two-dimensional (2D) site frequency spectrum (SFS) with the command *realSFS -fold* 1. Weighted F_{ST} estimates were calculated using the *realSFS fst* command and the 2D SFS as a prior. We considered outliers to be any window with an F_{ST} value of 5 SDs above the genome-wide mean. This analysis was performed across all 21 pairwise population comparisons, and results were plotted using the R package qqman (*90*). To avoid biases in the calculation of the genome-wide mean F_{ST}, we removed the sex chromosomes that exhibited lower effective population size (N_e) and higher overall F_{ST} values when compared to autosomal chromosomes.

GO enrichment

To better understand the functional implications of our candidate genes, we conducted a GO term enrichment analysis. This allowed us to identify any overrepresented biological functions or molecular pathways in our set of candidate genes. We obtained gene information for both Downy and Hairy Woodpeckers from the gene annotation of the Downy Woodpecker [NCBI RefSeq GCF_000699005.1 (*91*)]. To ensure the accuracy and reliability of our results, we used PANNZER2 (*92*) to extract GO terms directly from the full list of 15,137 annotated proteins in Downy Woodpecker based on homology searches in the UniProt database (*93*). We then performed a Fisher′s exact test in R (R Core Team 2020) to compare the number of candidate genes annotated with a certain GO term versus the total number of genes with that specific GO term annotation in the entire gene dataset. We considered a *P* value of significance of 0.05 after a false discovery rate correction for multiple testing.

Test for adaptive introgression

To test the hypothesis of adaptive introgression, we used a gene tree estimation approach to identify genomic regions that may have undergone introgression between Downy and Hairy Woodpeckers. We selected one individual (with the highest coverage) from each population ($n = 7$ per species) and phased and imputed their genotypes using Beagle 4 (*83*). Next, we used Phyml (*94*) to estimate neighbor-joining trees for windows of 100 SNPs across the genome. We then used Twisst (*95*) to calculate topology weights for each 100-SNP window and identify the topology with the highest support. We evaluated three topologies (T) based on (*18*): (T1) species are monophyletic, meaning that samples in a species form a clade; (T2) samples from the East are more closely related, regardless of species identity; and (T3) samples from the East in Downy Woodpecker are more closely related to samples from the West in Hairy Woodpecker and vice versa. We considered the genomic regions with the highest support for topologies 2 and 3

candidates of introgression. After identifying potential introgressed regions, we investigated whether they overlapped with our set of candidate genes under selection.

Supplementary Materials

This PDF file includes:

Figs. S1 to S11

Tables S1 to S7

View/request a protocol for this paper from *Bio-protocol*.

REFERENCES AND NOTES

1. A. E. Lobkovsky, E. V. Koonin, Replaying the tape of life: Quantification of the predictability of evolution. *Front. Genet.* **3**, 246 (2012).
2. V. Orgogozo, B. Morizot, A. Martin, The differential view of genotype-phenotype relationships. *Front. Genet.* **6**, 179 (2015).
3. E. B. Rosenblum, C. E. Parent, E. E. Brandt, The molecular basis of phenotypic convergence. *Annu. Rev. Ecol. Evol. Syst.* **45**, 203–226 (2014).
4. D. L. Stern, V. Orgogozo, The loci of evolution: How predictable is genetic evolution? *Evolution* **62**, 2155–2177 (2008).
5. G. L. Conte, M. E. Arnegard, C. L. Peichel, D. Schluter, The probability of genetic parallelism and convergence in natural populations. *Proc. R. Soc. B* **279**, 5039–5047 (2012).
6. J. A. Holliday, L. Zhou, R. Bawa, M. Zhang, R. W. Oubida, Evidence for extensive parallelism but divergent genomic architecture of adaptation along altitudinal and latitudinal gradients in *Populus trichocarpa*. *New Phytol.* **209**, 1240–1251 (2016).
7. M. Yuan, J. R. Stinchcombe, Population genomics of parallel adaptation. *Mol. Ecol.* **29**, 4033–4036 (2020).
8. B. A. Fraser, J. R. Whiting, What can be learned by scanning the genome for molecular convergence in wild populations? *Ann. N. Y. Acad. Sci.* **1476**, 23–42 (2020).
9. N. Walden, K. Lucek, Y. Willi, Lineage-specific adaptation to climate involves flowering time in North American *Arabidopsis lyrata*. *Mol. Ecol.* **29**, 1436–1451 (2020).
10. P. A. Hohenlohe, S. Bassham, P. D. Etter, N. Stiffler, E. A. Johnson, W. A. Cresko, Population genomics of parallel adaptation in threespine stickleback using sequenced RAD tags. *PLOS Genet.* **6**, e1000862 (2010).
11. J. E. Pool, D. T. Braun, J. B. Lack, Parallel evolution of cold tolerance within *Drosophila melanogaster*. *Mol. Biol. Evol.* **34**, 349–360 (2016).
12. J. Walsh, P. M. Benham, P. E. Deane-Coe, P. Arcese, B. G. Butcher, Y. L. Chan, Z. A. Cheviron, C. S. Elphick, A. I. Kovach, B. J. Olsen, W. G. Shriver, V. L. Winder, I. J. Lovette, Genomics of rapid ecological divergence and parallel adaptation in four tidal marsh sparrows. *Evol. Lett.* **3**, 324–338 (2019).
13. S. Lamichhaney, A. P. Fuentes-Pardo, N. Rafati, N. Ryman, G. R. McCracken, C. Bourne, R. Singh, D. E. Ruzzante, L. Andersson, Parallel adaptive evolution of geographically distant herring populations on both sides of the North Atlantic Ocean. *Proc. Natl. Acad. Sci. U.S.A.* **114**, E3452–E3461 (2017).
14. I. S. Magalhaes, J. R. Whiting, D. D'Agostino, P. A. Hohenlohe, M. Mahmud, M. A. Bell, S. Skúlason, A. D. C. MacColl, Intercontinental genomic parallelism in multiple three-spined stickleback adaptive radiations. *Nat. Ecol. Evol.* **5**, 251–261 (2021).
15. G.-D. Wang, W. Zhai, H.-C. Yang, R.-X. Fan, X. Cao, L. Zhong, L. Wang, F. Liu, H. Wu, L.-G. Cheng, A. D. Poyarkov, N. A. Poyarkov, S.-S. T. JR, W.-M. Zhao, Y. Gao, X.-M. Lv, D. M. Irwin, P. Savolainen, C.-I. Wu, Y.-P. Zhang, The genomics of selection in dogs and the parallel evolution between dogs and humans. *Nat. Commun.* **4**, 1860 (2013).
16. S. Yeaman, K. A. Hodgins, K. E. Lotterhos, H. Suren, S. Nadeau, J. C. Degner, K. A. Nurkowski, P. Smets, T. Wang, L. K. Gray, K. J. Liepe, A. Hamann, J. A. Holliday, M. C. Whitlock, L. H. Rieseberg, S. N. Aitken, Convergent local adaptation to climate in distantly related conifers. *Science* **353**, 1431–1433 (2016).
17. H. R. Ouellet, *Biosystematics and Ecology of Picoides villosus (L.) and P. pubescens (L.) (Aves Picidae)* (McGill University, 1977).
18. L. R. Moreira, J. Klicka, B. T. Smith, Demography and linked selection interact to shape the genomic landscape of codistributed woodpeckers during the Ice Age. *Mol. Ecol.* **32**, 1739–1759 (2023).
19. M. J. Dufort, An augmented supermatrix phylogeny of the avian family Picidae reveals uncertainty deep in the family tree. *Mol. Phylogenet. Evol.* **94**, 313–326 (2016).
20. S. B. Shakya, J. Fuchs, J.-M. Pons, F. H. Sheldon, Tapping the woodpecker tree for evolutionary insight. *Mol. Phylogenet. Evol.* **116**, 182–191 (2017).
21. A. C. Weibel, W. S. Moore, Plumage convergence in Picoides woodpeckers based on a molecular phylogeny, with emphasis on convergence in Downy and Hairy woodpeckers. *Condor* **107**, 797–809 (2005).
22. R. O. Prum, L. Samuelson, The Hairy–Downy game: A model of interspecific social dominance mimicry. *J. Theor. Biol.* **313**, 42–60 (2012).
23. M. Lammertink, C. Kopuchian, H. B. Brandl, P. L. Tubaro, H. Winkler, A striking case of deceptive woodpecker colouration: The threatened Helmeted Woodpecker Dryocopus galeatus belongs in the genus Celeus. *J. Ornithol.* **157**, 109–116 (2016).
24. E. T. Miller, G. M. Leighton, B. G. Freeman, A. C. Lees, R. A. Ligon, Ecological and geographical overlap drive plumage evolution and mimicry in woodpeckers. *Nat. Commun.* **10**, 1602 (2019).
25. J. M. Fernández, J. I. Areta, M. Lammertink, Does foraging competition drive plumage convergence in three look-alike Atlantic Forest woodpecker species? *J. Ornithol.* **161**, 1105–1116 (2020).
26. J. C. Cooper, Niche theory and its relation to morphology and phenotype in geographic space: A case study in woodpeckers (Picidae). *J. Avian Biol.* **49**, e01771 (2018).
27. A. L. Rand, Some size gradients in North American birds. *Wilson Bull.* **73**, 46–56 (1961).
28. F. C. James, Geographic size variation in birds and its relationship to climate. *Ecology* **51**, 365–390 (1970).
29. S. Hoban, J. L. Kelley, K. E. Lotterhos, M. F. Antolin, G. Bradburd, D. B. Lowry, M. L. Poss, L. K. Reed, A. Storfer, M. C. Whitlock, Finding the genomic basis of local adaptation: Pitfalls, practical solutions, and future directions. *Am. Nat.* **188**, 379–397 (2016).
30. J. Steen, Climatic adaptation in some small northern birds. *Ecology* **39**, 625–629 (1958).
31. E. T. Liknes, D. L. Swanson, Seasonal variation in cold tolerance, basal metabolic rate, and maximal capacity for thermogenesis in White-Breasted Nuthatches *Sitta carolinensis* and Downy Woodpeckers *Picoides pubescens*, two unrelated arboreal temperate residents. *J. Avian Biol.* **27**, 279–288 (1996).
32. S. C. Kendeigh, C. R. Blem, Metabolic adaptation to local climate in birds. *Comp. Biochem. Physiol. A Physiol.* **48**, 175–187 (1974).
33. D. L. Swanson, A comparative analysis of thermogenic capacity and cold tolerance in small birds. *J. Exp. Biol.* **209**, 466–474 (2006).
34. T. H. Hamilton, The adaptive significances of intraspecific trends of variation in wing length and body size among bird species. *Evolution* **15**, 180 (1961).
35. B. K. McNab, On the ecological significance of Bergmann's rule. *Ecology* **52**, 845–854 (1971).
36. T. H. Booth, H. A. Nix, J. R. Busby, M. F. Hutchinson, BIOCLIM: The first species distribution modelling package, its early applications and relevance to most current MAXENT studies. *Divers. Distrib.* **20**, 1–9 (2014).
37. E. Jørsboe, A. Albrechtsen, *Efficient approaches for large-scale GWAS with genotype uncertainty*, *G3* **12**, jkab385 (2022).
38. Y. Bourgeois, S. Boissinot, Selection at behavioural, developmental and metabolic genes is associated with the northward expansion of a successful tropical colonizer. *Mol. Ecol.* **28**, 3523–3543 (2019).
39. J. M. Jackson, M. L. Pimsler, K. J. Oyen, J. P. Strange, M. E. Dillon, J. D. Lozier, Local adaptation across a complex bioclimatic landscape in two montane bumble bee species. *Mol. Ecol.* **29**, 920–939 (2020).
40. J. Meisner, A. Albrechtsen, K. Hanghøj, Detecting selection in low-coverage high-throughput sequencing data using principal component analysis. *BMC Bioinformatics* **22**, 470 (2021).
41. Messer Lab website, *Messer lab website* (2014); https://messerlab.org/resources/.
42. T. S. Korneliussen, A. Albrechtsen, R. Nielsen, ANGSD: Analysis of next generation sequencing data. *BMC Bioinformatics* **15**, 356 (2014).
43. C. Bonneaud, S. L. Balenger, J. Zhang, S. V. Edwards, G. E. Hill, Innate immunity and the evolution of resistance to an emerging infectious disease in a wild bird. *Mol. Ecol.* **21**, 2628–2639 (2012).
44. H. Prüter, M. Franz, S. Twietmeyer, N. Böhm, G. Middendorff, R. Portas, J. Melzheimer, H. Kolberg, G. von Samson-Himmelstjerna, A. D. Greenwood, D. Lüschow, K. Mühldorfer, G. Á. Czirják, Increased immune marker variance in a population of invasive birds. *Sci. Rep.* **10**, 21764 (2020).
45. A. J. Shultz, T. B. Sackton, Immune genes are hotspots of shared positive selection across birds and mammals. *eLife* **8**, e41815 (2019).
46. Y. Bourgeois, S. Boissinot, On the population dynamics of junk: A review on the population genomics of transposable elements. *Genes* **10**, 419 (2019).
47. J. D. Manthey, R. G. Moyle, S. Boissinot, Multiple and independent phases of transposable element amplification in the genomes of Piciformes (woodpeckers and allies). *Genome Biol. Evol.* **10**, 1445–1456 (2018).
48. J. González, T. L. Karasov, P. W. Messer, D. A. Petrov, Genome-wide patterns of adaptation to temperate environments associated with transposable elements in Drosophila. *PLOS Genet.* **6**, e1000905 (2010).

49. G. Barnea, W. Strapps, G. Herrada, Y. Berman, J. Ong, B. Kloss, R. Axel, K. J. Lee, The genetic design of signaling cascades to record receptor activation. *Proc. Natl. Acad. Sci. U.S.A.* **105**, 64–69 (2008).
50. J. Röhrl, D. Yang, J. J. Oppenheim, T. Hehlgans, Specific binding and chemotactic activity of mBD4 and its functional orthologue hBD2 to CCR6-expressing cells. *J. Biol. Chem.* **285**, 7028–7034 (2010).
51. K. D. Kohl, P. Brzęk, E. Caviedes-Vidal, W. H. Karasov, Pancreatic and intestinal carbohydrases are matched to dietary starch level in wild passerine birds. *Physiol. Biochem. Zool.* **84**, 195–203 (2011).
52. Y.-H. Chen, H. Zhao, Evolution of digestive enzymes and dietary diversification in birds. *PeerJ.* **7**, e6840 (2019).
53. M. Ravinet, T. O. Elgvin, C. Trier, M. Aliabadian, A. Gavrilov, G.-P. Sætre, Signatures of human-commensalism in the house sparrow genome. *Proc. R. Soc. B.* **285**, 20181246 (2018).
54. K. Mann, M. Mann, The chicken egg yolk plasma and granule proteomes. *Proteomics* **8**, 178–191 (2008).
55. J. B. Allard, C. Duan, IGF-binding proteins: Why do they exist and why are there so many? *Front. Endocrinol.* **9**, 117 (2018).
56. H. Zhou, A. D. Mitchell, J. P. McMurtry, C. M. Ashwell, S. J. Lamont, Insulin-like growth factor-I gene polymorphism associations with growth, body composition, skeleton integrity, and metabolic traits in chickens. *Poult. Sci.* **84**, 212–219 (2005).
57. A. Hellström, D. Ley, I. Hansen-Pupp, B. Hallberg, L. A. Ramenghi, C. Löfqvist, L. E. H. Smith, A.-L. Hård, Role of insulin like growth factor 1 in fetal development and in the early postnatal life of premature infants. *Am. J. Perinatol.* **33**, 1067–1071 (2016).
58. S. N. Rajpathak, M. J. Gunter, J. Wylie-Rosett, G. Y. F. Ho, R. C. Kaplan, R. Muzumdar, T. E. Rohan, H. D. Strickler, The role of insulin-like growth factor-I and its binding proteins in glucose homeostasis and type 2 diabetes. *Diabetes Metab. Res. Rev.* **25**, 3–12 (2009).
59. A. Otto, K. Patel, Signalling and the control of skeletal muscle size. *Exp. Cell Res.* **316**, 3059–3066 (2010).
60. S. Mohan, C. Kesavan, Role of insulin-like growth factor-1 in the regulation of skeletal growth. *Curr. Osteoporos. Rep.* **10**, 178–186 (2012).
61. G.-S. Wang, H.-H. Liu, L.-S. Li, J.-W. Wang, Influence of ovo injecting IGF-1 on weights of embryo, heart and liver of duck during hatching stages. *Int. J. Poult. Sci.* **11**, 756–760 (2012).
62. J. Lodjak, M. Mägi, V. Tilgar, Insulin-like growth factor 1 and growth rate in nestlings of a wild passerine bird. *Funct. Ecol.* **28**, 159–166 (2014).
63. J. Lodjak, M. Mägi, E. Sild, R. Mänd, Causal link between insulin-like growth factor 1 and growth in nestlings of a wild passerine bird. *Funct. Ecol.* **31**, 184–191 (2017).
64. J. Lodjak, R. Mänd, M. Mägi, Insulin-like growth factor 1 and life-history evolution of passerine birds. *Funct. Ecol.* **32**, 313–323 (2018).
65. K. Mahr, O. Vincze, Z. Tóth, H. Hoi, Á. Z. Lendvai, Insulin-like growth factor 1 is related to the expression of plumage traits in a passerine species. *Behav. Ecol. Sociobiol.* **74**, 39 (2020).
66. C. Bergmann, About the relationships between heat conservation and body size of animals. *Goett Stud.* **1**, 595–708 (1847).
67. K. G. Ashton, Patterns of within-species body size variation of birds: Strong evidence for Bergmann's rule. *Glob. Ecol. Biogeogr.* **11**, 505–523 (2002).
68. V. A. Olson, R. G. Davies, C. D. L. Orme, G. H. Thomas, S. Meiri, T. M. Blackburn, K. J. Gaston, I. P. F. Owens, P. M. Bennett, Global biogeography and ecology of body size in birds. *Ecol. Lett.* **12**, 249–259 (2009).
69. J. F. Storz, *Hemoglobin: Insights into Protein Structure, Function, and Evolution* (Oxford Univ. Press, 2018).
70. J. C. Opazo, F. G. Hoffmann, C. Natarajan, C. C. Witt, M. Berenbrink, J. F. Storz, Gene turnover in the avian globin gene families and evolutionary changes in hemoglobin isoform expression. *Mol. Biol. Evol.* **32**, 871–887 (2015).
71. S. C. Galen, C. Natarajan, H. Moriyama, R. E. Weber, A. Fago, P. M. Benham, A. N. Chavez, Z. A. Cheviron, J. F. Storz, C. C. Witt, Contribution of a mutational hot spot to hemoglobin adaptation in high-Altitude Andean house wrens. *Proc. Natl. Acad. Sci. U.S.A.* **112**, 13958–13963 (2015).
72. C. Natarajan, F. G. Hoffmann, R. E. Weber, A. Fago, C. C. Witt, J. F. Storz, Predictable convergence in hemoglobin function has unpredictable molecular underpinnings. *Science* **354**, 336–339 (2016).
73. M. Damek-Poprawa, T. Diemer, V. S. Lopes, C. Lillo, D. C. Harper, M. S. Marks, Y. Wu, J. R. Sparrow, R. A. Rachel, D. S. Williams, K. Boesze-Battaglia, Melanoregulin (MREG) modulates lysosome function in pigment epithelial cells. *J. Biol. Chem.* **284**, 10877–10889 (2009).
74. N. Ohbayashi, Y. Maruta, M. Ishida, M. Fukuda, Melanoregulin regulates retrograde melanosome transport through interaction with the RILP-p150^{Glued} complex in melanocytes. *J. Cell Sci.* **125**, 1508–1518 (2012).
75. C. S. Ng, W.-H. Li, Genetic and molecular basis of feather diversity in birds. *Genome Biol. Evol.* **10**, 2572–2586 (2018).
76. A. M. Bolger, M. Lohse, B. Usadel, Trimmomatic: A flexible trimmer for Illumina sequence data. *Bioinformatics* **30**, 2114–2120 (2014).
77. S. Andrews, FastQC: A quality control tool for high throughput sequence data [Online Software] (2010).
78. H. Li, R. Durbin, Fast and accurate short read alignment with Burrows-Wheeler transform. *Bioinformatics* **25**, 1754–1760 (2009).
79. A. McKenna, M. Hanna, E. Banks, A. Sivachenko, K. Cibulskis, A. Kernytsky, K. Garimella, D. Altshuler, S. Gabriel, M. Daly, M. A. DePristo, The genome analysis toolkit: A MapReduce framework for analyzing next-generation DNA sequencing data. *Genome Res.* **20**, 1297–1303 (2010).
80. K. Okonechnikov, A. Conesa, F. García-Alcalde, Qualimap 2: Advanced multi-sample quality control for high-throughput sequencing data. *Bioinformatics* **32**, 292–294 (2016).
81. M. A. DePristo, E. Banks, R. Poplin, K. V. Garimella, J. R. Maguire, C. Hartl, A. A. Philippakis, G. del Angel, M. A. Rivas, M. Hanna, A. McKenna, T. J. Fennell, A. M. Kernytsky, A. Y. Sivachenko, K. Cibulskis, S. B. Gabriel, D. Altshuler, M. J. Daly, A framework for variation discovery and genotyping using next-generation DNA sequencing data. *Nat. Genet.* **43**, 491–498 (2011).
82. P. Cingolani, A. Platts, L. L. Wang, M. Coon, T. Nguyen, L. Wang, S. J. Land, X. Lu, D. M. Ruden, A program for annotating and predicting the effects of single nucleotide polymorphisms, SnpEff. *Fly* **6**, 80–92 (2012).
83. S. R. Browning, B. L. Browning, Rapid and accurate haplotype phasing and missing-data inference for whole-genome association studies by use of localized haplotype clustering. *Am. J. Hum. Genet.* **81**, 1084–1097 (2007).
84. L. Skotte, T. S. Korneliussen, A. Albrechtsen, Estimating individual admixture proportions from next generation sequencing data. *Genetics* **195**, 693–702 (2013).
85. T. R. Booker, S. Yeaman, M. C. Whitlock, The WZA: A window-based method for characterizing genotype-environment association. *bioRxiv*, 2021.06.25.449972 (2021).
86. G. Montejo-Kovacevich, P. A. Salazar, S. H. Smith, K. Gavilanes, C. N. Bacquet, Y. F. Chan, C. D. Jiggins, J. I. Meier, N. J. Nadeau, Genomics of altitude-associated wing shape in two tropical butterflies. *Mol. Ecol.* **30**, 6387–6402 (2021).
87. H. Tavares, *WindowScanR* [R package] (2016); https://github.com/tavareshugo/WindowScanR.
88. P. Danecek, A. Auton, G. Abecasis, C. A. Albers, E. Banks, M. A. DePristo, R. E. Handsaker, G. Lunter, G. T. Marth, S. T. Sherry, G. McVean, R. Durbin, The variant call format and VCFtools. *Bioinformatics* **27**, 2156–2158 (2011).
89. S. Y. Kim, K. E. Lohmueller, A. Albrechtsen, Y. Li, T. Korneliussen, G. Tian, N. Grarup, T. Jiang, G. Andersen, D. Witte, T. Jorgensen, T. Hansen, O. Pedersen, J. Wang, R. Nielsen, Estimation of allele frequency and association mapping using next-generation sequencing data. *BMC Bioinformatics* **12**, 231 (2011).
90. S. D. Turner, qqman: An R package for visualizing GWAS results using Q-Q and manhattan plots, in *Cold Spring Harbor Laboratory* (2014), p. 005165.
91. E. D. Jarvis, S. Mirarab, A. J. Aberer, B. B. Li, P. Houde, C. Li, E. Al., S. Y. W. Ho, B. C. Faircloth, B. Nabholz, J. T. Howard, A. Suh, C. C. Weber, R. R. da Fonseca, J. Li, F. Zhang, H. Li, L. Zhou, N. Narula, L. Liu, G. Ganapathy, B. Boussau, M. S. Bayzid, V. Zavidovych, S. Subramanian, T. Gabaldon, S. Capella-Gutierrez, J. Huerta-Cepas, B. Rekepalli, K. Munch, M. Schierup, B. Lindow, W. C. Warren, D. Ray, R. E. Green, M. W. Bruford, X. Zhan, A. Dixon, S. Li, N. Li, Y. Huang, E. P. Derryberry, M. F. Bertelsen, F. H. Sheldon, R. T. Brumfield, C. V. Mello, P. V. Lovell, M. Wirthlin, M. P. C. Schneider, F. Prosdocimi, J. A. Samaniego, A. M. V. Velazquez, A. Alfaro-Nunez, P. F. Campos, B. Petersen, T. Sicheritz-Ponten, A. Pas, T. Bailey, P. Scofield, M. Bunce, D. M. Lambert, Q. Zhou, P. Perelman, A. C. Driskell, B. Shapiro, Z. Xiong, Y. Zeng, S. Liu, Z. Li, B. Liu, K. Wu, J. Xiao, X. Yinqi, Q. Zheng, Y. Zhang, H. Yang, J. Wang, L. Smeds, F. E. Rheindt, M. Braun, J. Fjeldsa, L. Orlando, F. K. Barker, K. A. Jonsson, W. Johnson, K.-P. Koepfli, S. O'Brien, D. Haussler, O. A. Ryder, C. Rahbek, E. Willerslev, G. R. Graves, T. C. Glenn, J. McCormack, D. Burt, H. Ellegren, P. Alstrom, S. V. Edwards, A. Stamatakis, D. P. Mindell, J. Cracraft, E. L. Braun, T. Warnow, W. Jun, M. T. P. Gilbert, G. Zhang, E. Al., Whole-genome analyses resolve early branches in the tree of life of modern birds. *Science* **346**, 1320–1331 (2014).
92. P. Törönen, A. Medlar, L. Holm, PANNZER2: A rapid functional annotation web server. *Nucleic Acids Res.* **46**, W84–W88 (2018).
93. A. Bateman, M.-J. Martin, S. Orchard, M. Magrane, R. Agivetova, S. Ahmad, E. Alpi, E. H. Bowler-Barnett, R. Britto, B. Bursteinas, Others, UniProt: The universal protein knowledgebase in 2021. *Nucleic Acids Res.* **49**, D480–D489 (2021).
94. S. Guindon, J.-F. Dufayard, V. Lefort, M. Anisimova, W. Hordijk, O. Gascuel, New algorithms and methods to estimate maximum-likelihood phylogenies: Assessing the performance of PhyML 3.0. *Syst. Biol.* **59**, 307–321 (2010).
95. S. H. Martin, S. M. Van Belleghem, Exploring evolutionary relationships across the genome using topology weighting. *Genetics* **206**, 429–438 (2017).

Acknowledgments: We thank the following individuals and institutions for providing tissue samples and specimen loans for this study: J. Klicka, S. Birk, and R. Faucett (University of Washington Burke Museum); C. M. Milensky (Smithsonian Institution); G. Spellman and A. Doll (Denver Museum of Nature & Science); C. Dardia (Cornell University Museum of Vertebrates); B. Marks, S. Hackett, and J. Bates (Field Museum of Natural History); K. Barker and T. Imfeld (Midwest Museum of Natural History); F. Sheldon and D. Dittmann (LSU Museum of Natural Science); and C. Witt, A. Johnson, and M. Anderson (Museum of Southwestern Biology). We also thank M. Brady, L. DeCicco, and P. Sweet for their assistance in collecting samples in the field. We lastly thank K. Provost, V. Chua, J. Merwin, G. Seehozer, G. Thom, W. Mauck, E. Tenorio, L. Musher, A. Rocha, B. Almeida, L. Coelho, I. Overcast, T. Trombone, J. Cracraft, M. Przeworski, F. Burbrink, D. Eaton, and D. Melnick for intellectual contribution during the development and writing of this manuscript. We also thank two anonymous reviewers whose suggestions substantially improved the quality of this work. **Funding:** This study was supported by the Department of Ecology, Evolution, and Environmental Biology (E3B) at Columbia University, Conselho Nacional de Desenvolvimento Científico e Tecnológico (CNPq; grant no. 211496/2014-6; grantee: L.R.M.), the Frank M. Chapman Memorial Fund and Linda J. Gormezano Memorial Fund from the American Museum of Natural History (AMNH), the American Ornithological Society Hesse Award, the Society of Systematic Biologists Graduate Student Research Award, and a U.S. National Science Foundation (DEB-1655736; grantee: B.T.S.). **Author contributions:** Conceptualization: L.R.M. and B.T.S. Methodology: L.R.M. and B.T.S. Investigation: L.R.M. Visualization: L.R.M. Supervision: B.T.S. Writing—original draft: L.R.M. Writing—review and editing: L.R.M. and B.T.S. **Competing interests:** The authors declare that they have no competing interests. **Data and materials availability:** All data needed to evaluate the conclusions in the paper are present in the paper and/or the Supplementary Materials. Whole-genome resequencing data are available on the Sequence Read Archive (https://ncbi.nlm.nih.gov/sra) under the BioProject PRJNA917637. Genome-wide F_{ST}, H, and LRT estimates are available on Dryad (doi: 10.5061/dryad.6m905qg42). The code used for this study can be found on Zenodo (doi: 10.5281/zenodo.7510791) and GitHub (https://github.com/lucasrocmoreira/Moreira-Smith_SciAdv_2023).

Submitted 17 May 2022
Accepted 17 April 2023
Published 19 May 2023
10.1126/sciadv.add0560

Science Advances

Convergent genomic signatures of local adaptation across a continental-scale environmental gradient

Lucas R. Moreira and Brian Tilston Smith

Sci. Adv., **9** (20), eadd0560.
DOI: 10.1126/sciadv.add0560

Science Advances (ISSN) is published by the American Association for the Advancement of Science. 1200 New York Avenue NW, Washington, DC 20005. The title *Science Advances* is a registered trademark of AAAS.